

**CALIBRATION OF THE FREQUENCIES OF STELLAR
SPECTRAL LINES**

A Senior Scholars Thesis

by

JUANA GOMEZ

Submitted to the Office of Undergraduate Research
Texas A&M University
in partial fulfillment of the requirements for the designation as

UNDERGRADUATE RESEARCH SCHOLAR

April 2010

Major: Physics

**CALIBRATION OF THE FREQUENCIES OF STELLAR
SPECTRAL LINES**

A Senior Scholars Thesis

by

JUANA GOMEZ

Submitted to the Office of Undergraduate Research
Texas A&M University
in partial fulfillment of the requirements for the designation as

UNDERGRADUATE RESEARCH SCHOLAR

Approved by:

Research Advisor:
Associate Dean for Undergraduate Research:

Edward S. Fry
Robert C. Webb

April 2010

Major: Physics

ABSTRACT

Calibration of the Frequencies of Stellar Spectral Lines. (April 2010)

Juana Gomez
Department of Physics
Texas A&M University

Research Advisor: Dr. Edward S. Fry
Department of Physics

When studying the expansion of the universe, a significant problem is measuring the red shifts of stellar absorption lines with sufficiently high accuracy; this requires extremely accurate reference frequencies for calibration. An important recent development is the use of laser frequency combs to provide the calibration frequencies. However, this approach is very time consuming and expensive. We are proposing a simple calibration approach using weak molecular absorption lines.

Our new approach is based on our recent development of a new diffuse reflecting surface whose reflectivity far exceeds anything previously available. Consider a basketball size cavity whose wall is made of this new diffuse reflector. Due to the high wall reflectivity, the effective absorption path length for light bouncing around inside this cavity is on the order of a kilometer. Consequently, even molecules with very weak absorption lines will show strong distinct absorption lines that can serve as calibration frequencies.

ACKNOWLEDGMENTS

My family has provided much support throughout my undergraduate career at TAMU. Everyone from my parents to the youngest of my nieces have also been an inspiration. In the physics department, Dr. Fry gave me the great opportunity to work in his lab. He has been a great example of passion, hard work, and creativity in physics research. Thanks to the responsibilities associated with this research, I explored deeper into the field of optics. Everyone in the lab has been helpful during this undergraduate experience: David Haubrich, Dr. Musser, and especially Michael Cone, who has provided tremendous guidance and support. This research project was conducted thanks to the partial funding of the Louis Stokes Alliance for Minority Participation (LSAMP). Everything has been given to me, may this be for the glory of God.

TABLE OF CONTENTS

	Page
ABSTRACT	iii
ACKNOWLEDGMENTS.....	iv
TABLE OF CONTENTS.....	v
LIST OF FIGURES	vi
CHAPTER	
I INTRODUCTION.....	1
II METHODS.....	5
Integrating cavity	5
Diffuse reflector.....	7
Experimental method	9
III RESULTS	11
IV SUMMARY AND CONCLUSIONS	15
REFERENCES	16
CONTACT INFORMATION	18

LIST OF FIGURES

FIGURE	Page
1 Fume silica agglomerates	8
2 Experimental arrangement.....	10
3 Three measurements.....	12
4 Integrating cavity instrument	13
5 Output.....	14

CHAPTER I

INTRODUCTION

High precision astronomical instruments are needed to solve crucial questions in astronomy. These questions deal with the existence of Earth-like planets and the expansion of the Universe¹. Currently, the methods astronomers use for detecting planets orbiting distant stars are only capable of finding very large and massive planets².

Each star has distinct absorption lines specific to the components of its atmosphere. When a planet orbits around a star, it causes the motion of the star to wobble. Thus, a change in the star's radial speed produces a shift in the frequencies observed. When the star travels towards Earth a redshift is observed; when it travels away from Earth a blueshift is seen. By analyzing the shifts in frequency, astronomers can calculate the star's distance from Earth and can infer the existence of planets. This also aids in obtaining valuable information about the expansion of the universe. However, to detect a planet the size of Earth orbiting a star the size of our sun, it would be necessary to measure changes in the radial speed of about 10 centimeters per second during a period of one year³. Our objective is the determination of these radial velocity changes via a

This thesis follows the style and format of Applied Optics.

calibration with molecular absorption lines in the range from 800 nm to 1100 nm.

The spectrum of light emitted from stars or galaxies contain a series of absorption lines. These lines mark the wavelengths where the gas in the star's atmosphere has absorbed light. A complete spectrum of a star provides information on the composition of the star's outer atmosphere. If a source of light is moving towards or away from the Earth with some radial velocity, there is a shift in the location of the absorption lines as observed from Earth. For relatively small velocities, the radial velocity of an object increases linearly with its distance. This provides a tool to measure the speeds of stars in our own Milky Way. Yet, when looking at objects outside our galaxy, the absorption lines shift by very large amounts.

The most accepted methods for measuring cosmological parameters depend on the accuracy of the luminosity distance to extragalactic sources with known redshifts. These methods, which make assumptions about the luminosity of the stellar sources, are often affected by the uncertainties in measurements or by evolutionary effects. As the universe accelerates, all cosmological objects are redshifted by a velocity of a few meters per second.⁴ A planet orbiting a star causes the star to wobble. The search for these small shifts in the motion of stars potentially caused by planets has led to the development of spectroscopic methods that result in radial velocities errors of $\sim 3\text{ms}^{-1}$.⁵ However, to take

advantage of the high velocity precision provided by echelle spectrographs, precise wavelength calibration is essential.⁶

The lack of higher precision instrumentation is compelling. The search for extra-solar planets using radial velocity measurements has reached a precision better than 1 ms^{-1} over the wavelength range between ~ 100 to 300 nm . Higher velocity precision potentially provides the possibility of measuring of the acceleration of the expansion of the universe.⁴

Several methods have been developed to improve measurements in radial velocities. One of these methods employs an echelle spectrograph and an iodine cell. The absorption lines of iodine provide a reference spectrum for measuring the shifts in the radial velocity of stars.⁵ The most common calibration technique is the thorium-argon (ThAr) hollow-cathode emission-line lamp, which is relatively cheap and has lines in the entire visual spectrum.⁶ However, these techniques provide several disadvantages. Iodine cells have very few spectral lines in the red and near- infrared spectral bands and absorb about half of the light from the source, significantly reducing the signal-to-noise ratio. Also, ThAr lines differ significantly in spacing and intensity. These lamps are specially unstable over long-time scales due to variations in current and pressure. The most significant development towards frequency calibration is the optical frequency combs.

Frequency combs use mode-locked femtosecond-pulsed to provide continuous modes.² However, this method requires the use of a Fabry-Pérot filtering cavity, making the calibration method complicated and expensive.

We are primarily concerned with frequency calibration for molecular absorption lines in the infrared region. This new calibration concept is based on our new diffuse reflector that has a very high reflectivity, the highest known for diffuse reflectors from the infrared down to 266 nm. The utilization of this material in an integrating cavity enhances the performance of the integrating cavity by increasing the path length by up to two orders of magnitude. The extremely long path lengths in the integrating cavity will produce sharp and strong absorption lines even for very weak absorbers.

CHAPTER II

METHODS

Integrating cavity

Integrating cavities have a wide use in commercial and experimental research for the measurements and collection of radiant flux from a source. They have the capability to collect all the emitted flux of a source, facilitating measurements of the total output of the source, as well as measurements of reflectance and transmittance. Integrating cavities have uses in different areas such as radiometry, spectroscopy, photometry, and materials characterization. They can be used with lasers as pump cavities or as sources of uniform illumination. Most importantly, integrating cavities provide a powerful tool for spectroscopy of weak absorbing media.⁷

The integrating cavity spatially integrates a radiant flux. When the wall reflectivity of an integrating cavity approaches unity, the decay of a temporarily short pulse in an empty cavity can provide a measurement of the absolute reflectivity of the cavity wall. Knowing the reflectivity of the integrating cavity wall allows extremely sensitive measurements of weak absorption.⁸ This is attained by monitoring the decaying field of a temporarily short pulse in the presence of a weakly absorbing medium.⁶ The time response of an integrating cavity is

$$E_i(t) = E_0 e^{-\frac{t}{\tau}} \quad (1)$$

where it is assumed that the irradiance incident on the walls $E_i(t)$ decays exponentially, and E_0 is the irradiance incident on the cavity walls at time $t=0$. After each reflection, the irradiance leaving the cavity wall E_L is the incident irradiance multiplied by the reflectivity ρ . If the irradiance incident on the walls at time t is $E_i(t)$, the irradiance leaving the cavity wall at time t is then

$$E_L(t) = \rho E_0 e^{-\frac{t}{\tau}}. \quad (2)$$

During a time t equal to the decay constant τ , there will be a number of reflections n . Two cases can be considered for the zero of time. The zero of time can be considered at the first reflection or it can be taken so that the first reflection occurs at the average time \bar{t} . For the first case (the zero time is chosen at the instant of the first reflection), the irradiance at the $(n + 1)^{\text{th}}$ reflection (when $t = n\bar{t} = \tau$) will be

$$E_i(\tau) = E_0 \rho^n, \quad E_L(\tau) = E_0 \rho^{n+1} \quad (3)$$

From (2) and (3), the irradiances at $t=\tau$ are

$$E_1(\tau) = \rho E_0 e^{-1}, \quad E_L(\tau) = E_0 \rho e^{-1}, \quad (4)$$

These expressions lead to

$$n = -\frac{1}{\ln \rho}, \quad \tau_i = -\frac{1}{\ln \rho} \bar{t} = \left(-\frac{1}{\ln \rho}\right) \left(\frac{d_{av}}{c}\right) \quad (5)$$

for E_i and E_L , where $\bar{t} = \frac{d_{av}}{c} \bar{t}$ was used for the average time. The subscript i has been added to identify this case.

At reflectivity $\rho=0$, Eq. (6) gives $n = 0$ and $\tau_i = n\bar{\tau} = 0$. This makes physical sense, since at time $t=0$, all the photons are incident on the wall and the reflectivity is zero. On the other extreme, for ρ near unity, n and τ_i will be large, also as expected.

In the second case, the zero time is chosen so that the first reflection occurs at the average time $\bar{\tau}$. Then, at the time of the n th reflection, $t = n\bar{\tau} = \tau$. This expression, combined with

$$n = -1/(\ln\rho), \quad \tau_{ii}=(1 - 1/\ln \rho) \bar{\tau}=(1-1/\ln \rho)(\bar{d}/c) \quad (6)$$

for both E_i and E_L . The subscript ii distinguishes this case. In this case, when the reflectivity $\rho=0$, Eq. (6) gives $n=1$ and $\tau_{ii}=\bar{\tau}$. At time $t=0$, photons must travel an average time $\bar{\tau}$ before hitting the wall, then τ_{ii} is expected to be $\approx \bar{\tau}$. For ρ near unity, n will be very large, and the difference between the results of the two different cases corresponding to Eq. (5) and (6) is insignificant. However, a Monte Carlo simulation of the time response was performed by Fry, et al. to determine the best assumption for the zero time. These simulations performed by Fry, et al. concluded that the best analytical approximation for the decay constant is Eq. (5).

Diffuse reflector

One of the key components of our new approach for the integrating cavity is fumed silica, a highly efficient diffuse reflector. Fumed silica, or quartz powder, is formed of small particles of about 40 nm naturally found in agglomerates of $\sim 8.5 \mu\text{m}$. (Musser)

The physical characteristics of such agglomerates make the powder easily manageable. Using pressure we can mold the powder into cylindrical, or other shapes depending of the purpose of our experiment. The interfaces between the quartz particles and the air produce a very high reflectivity, which dramatically improves the sensitivity of our integrating cavity.⁹ We used fumed silica EG50 in our integrating cavity experiment. Fig. 1 shows the image of a fumed silica agglomerate.

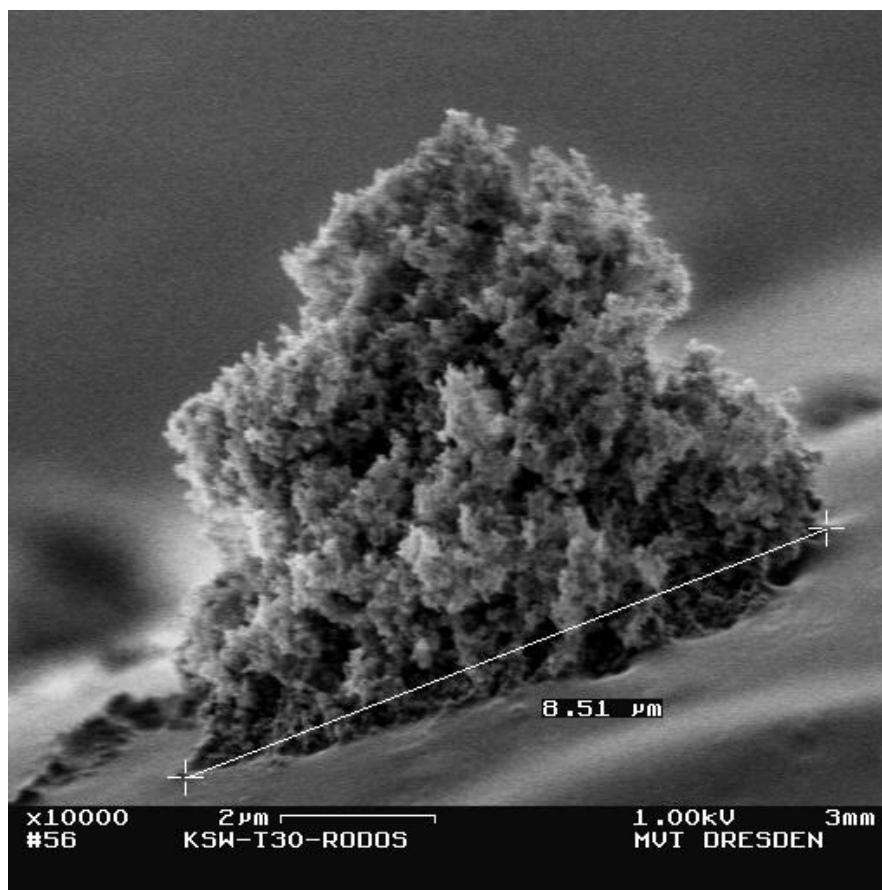


Fig.1. Fume silica agglomerate

Experimental method

The use of quartz powder for the walls of an integrating cavity can significantly improve the measurements of absorption coefficients especially in the case of severe scattering effects. Measurements of the reflectivity at 532 nm of a quartz powder wall give a wall reflectivity of .999; this means a cavity with such walls will be extremely sensitive to weak absorptions.⁹

The measurement of molecular absorption lines consists of sending light through an absorber, which is then detected by a spectrometer. Our input signal is provided by a 6271 Xenon-Mercury arc lamp. This light source covers a wide range of the spectrum, from 260 nm to 2400 nm. Most importantly, it provides spectral output in the near infrared (NIR); this is the wavelength range of interest for our calibration of weak stellar spectral lines.

The light source is incident on a monochromator, which selects the wavelengths supplied to the integrating cavity. The light is focused with the aid of two lenses. The cavity contains the gas, carbon monoxide, which provides absorption lines in the infrared. Upon entering the cavity, the light travels through the absorber and hits the walls of the cavity multiple times. After a period of time, some of the light exits through another quartz rod. This exiting rod is located in the wall of the cavity at an angle perpendicular to the first rod. The function of the exit rod is guiding the light to an ET type

photomultiplier tube, which is sensitive from 165nm to 900 nm. The experimental arrangement is shown in figure 2.

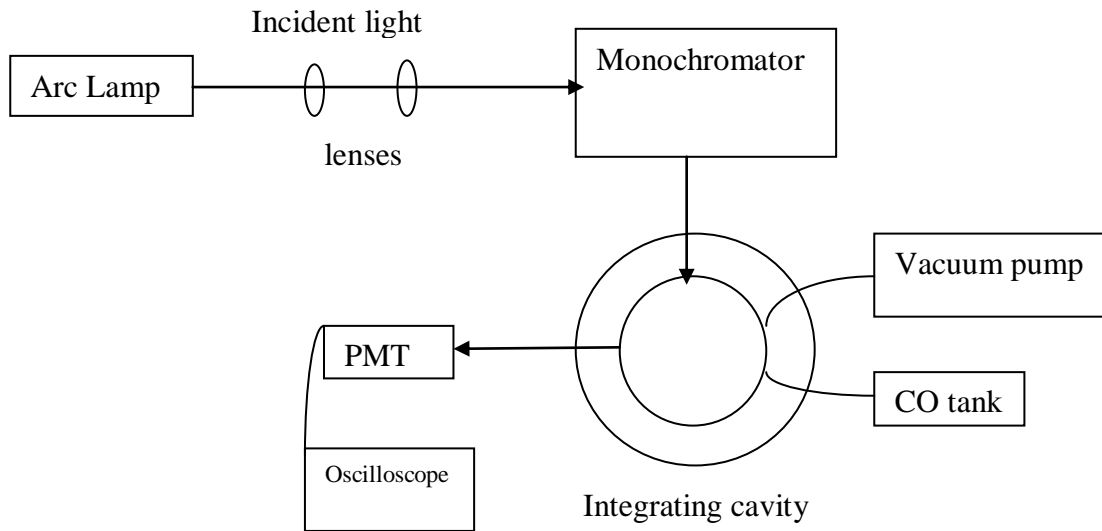


Fig. 2 Experimental arrangement

CHAPTER III

RESULTS

Multiple runs were performed with the purpose of testing the equipment before taking measurements using the integrating cavity. With the initial setup, a McPherson spectrometer was used to measure absorption of bromine in a wide range of wavelengths.

Figure 3 shows spectral lines of bromine. Light was sent through a bromine cell cooled to approximately three degrees Celsius. White Light-Emitting Diodes (LED's) were used as light input. Light traveled through the bromine cell. The blue line corresponds to the initial measurement of the signal traveling through air, which only shows an almost flat line. This is expected, since there is no absorption expected in the air. The other lines represent multiple runs of white LED light passing through the cold bromine cell.

To obtain the measurements at multiple wavelengths, a McPherson spectrometer was used. The calibration of the spectrometer was performed with a helium-neon laser. As shown in the figure, in general, the lines of each measurement coincide in the dips. Due to the poor wavelength resolution of the McPherson spectrometer, these dips correspond to absorption by multiple lines of bromine. The slight variations in the data result from the changing temperature between runs and minor voltage changes. These initial

measurements helped to determine the proper functioning of the equipment for use in subsequent runs.

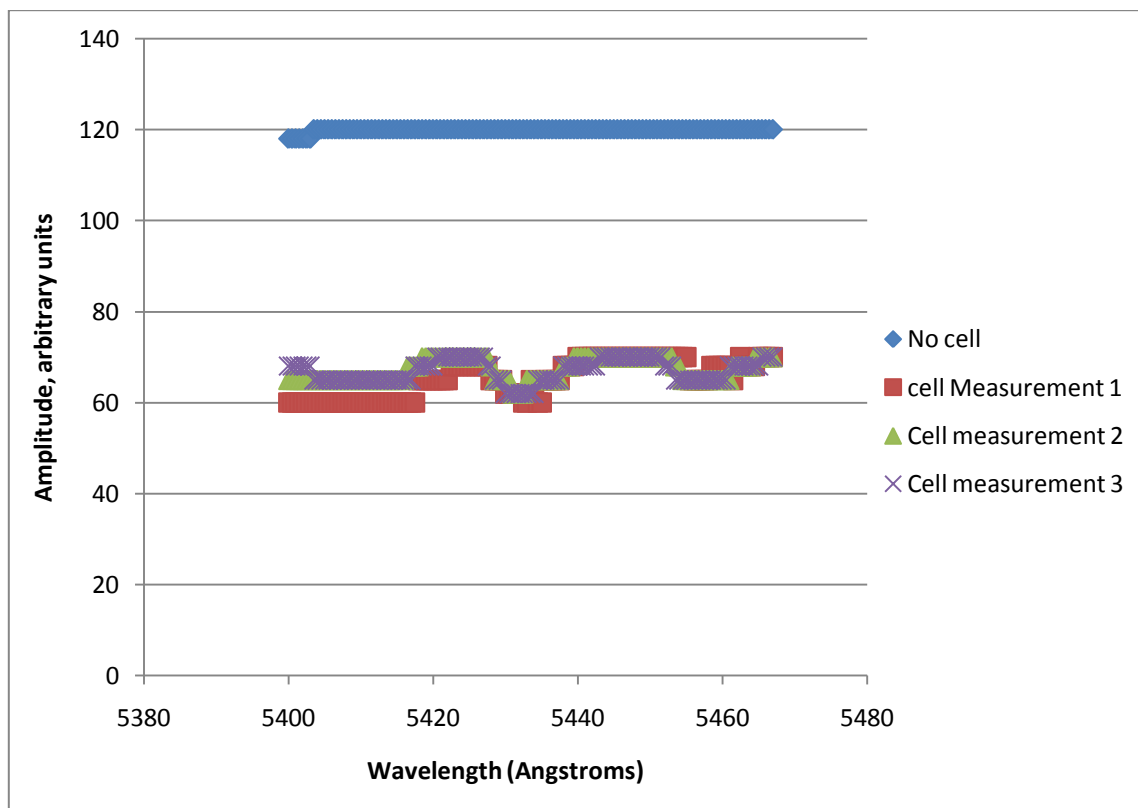


Figure 3. Three measurements of the absorption lines of a bromine cell. White LED's were used as light input. The dark blue line represents a measurement of the light in the region without the bromine cell. The colored lines show different measurements of the same region using a cold bromine cell.

We used a cylinder of PVC material, with metal plates at the ends for our integrating cavity. The outer diameter of the cylinder was 8.6 inches. A spherical quartz bulb with a diameter of 5.875 inches, was contained in the cylinder as our cavity. The quartz bulb was surrounded with Aerosil EG50, quartz powder, and then pressed with lead bricks.

Light was introduced into the cavity with a quartz rod. An identical quartz rod was placed 90° apart from the input quartz rod. The cylinders were inserted in the midpoint of the wall. Major features of the integrating cavity are shown in figure 4.

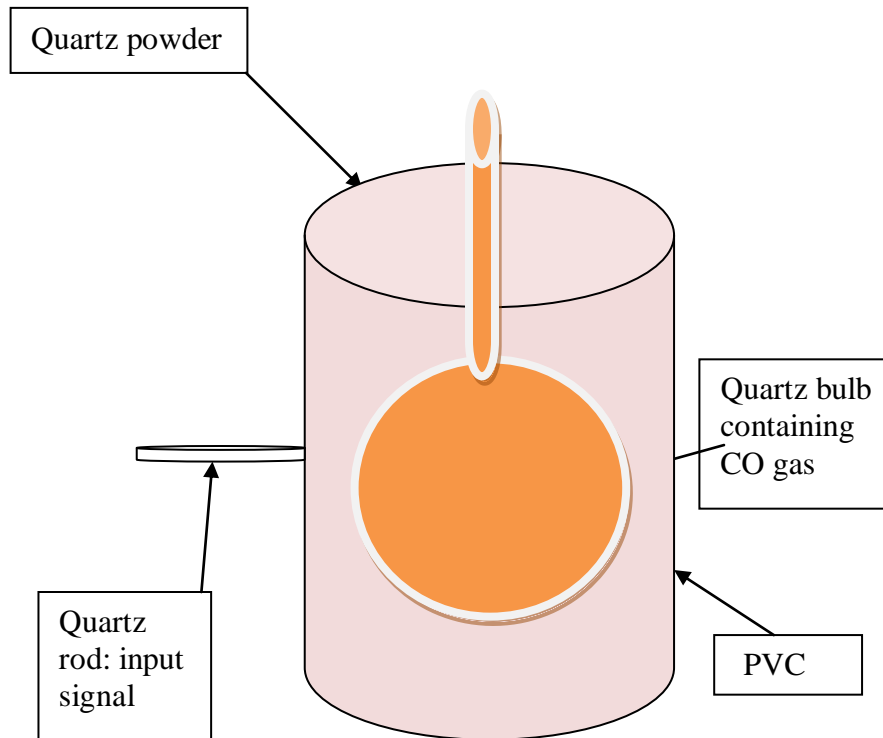


Figure 4. Integrating cavity instrument

Once the integrating cavity was completed and ready to be incorporated into the vacuum system, some runs were performed to test the reflectivity of the cavity walls. A pulse laser was used to perform these trials. Figure 5 shows the results of reflectivity tests for the integrating cavity.

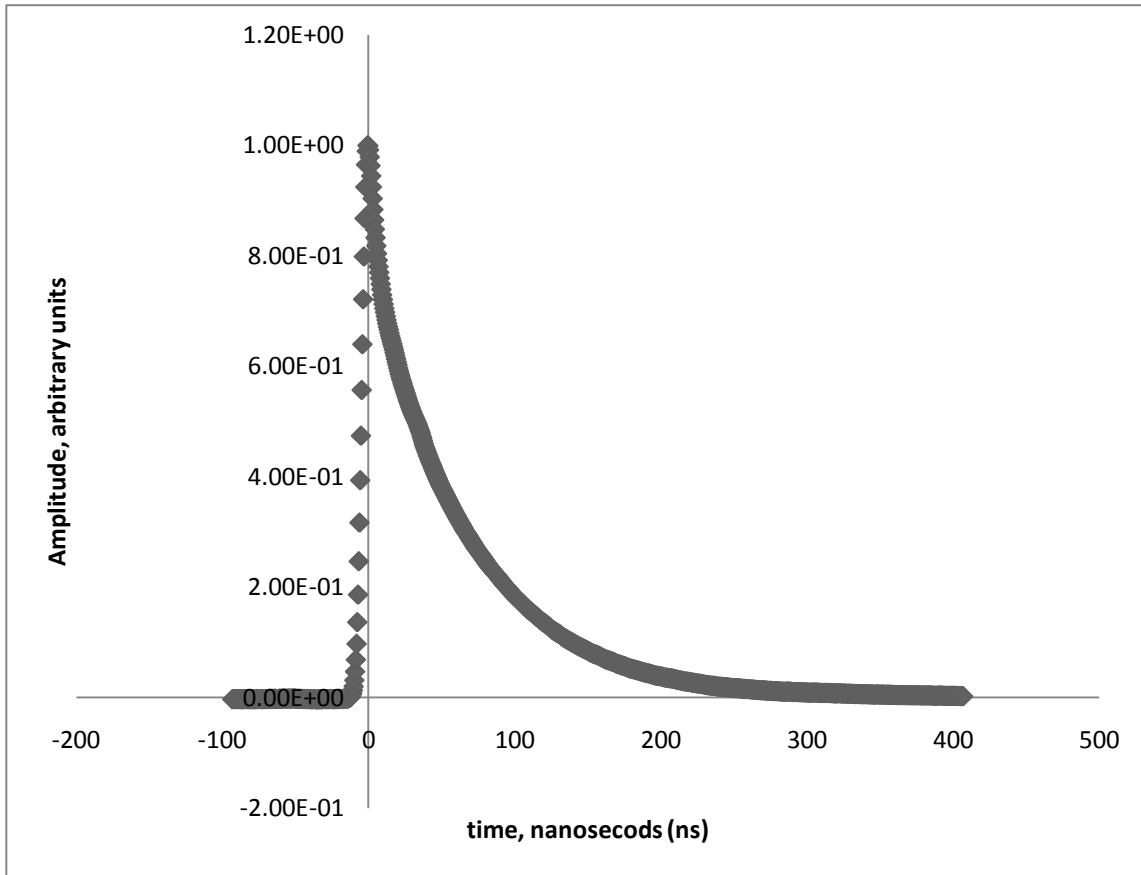


Figure 5. Output of the pulse's tail at 532 nm presents an exponential graph.

Laser pulses, at 532 nm from 10 to 20 ns wide, were introduced into the cavity. Fig 6 shows the cavity response at 532 nm as obtained from the oscilloscope trace of a single shot. At 532 nm the observed decay time is $\tau^{-1} = 0.0156 \text{ ns}^{-1}$. For this measurement and using the theory developed by Fry, et al., the average reflectivity is 0.99506. Higher reflectivity has been obtained previously due to sintering and baking of the powder. But, these results show that the reflectivity of the cavity walls will be very good for the present experiments.

CHAPTER IV

SUMMARY AND CONCLUSIONS

We have set up the instrumentation to measure the absorption of carbon monoxide in the near infrared. The measurements are based on the theory integrating cavities using a highly diffuse reflector. The high reflectivity of our integrating cavity should provide strong reference lines for the calibration of stellar spectra redshifted to the infrared.

REFERENCES

1. ESO, "A fine-tooth comb to measure the accelerating universe." ScienceDaily.4 September 2008.
<http://esciencenews.com/articles/2008/09/04/a.fine.tooth.comb.measure.accelerating.universe>.
2. C.H. Li, A.J. Benedick, P. Fendel, A.G. Glenday, F.X. Kärtner, *et al.*, "A laser frequency comb that enables radial velocity measurements with a precision of 1 cm s^{-1} ," Nature **452**, 610-612 (2008)
3. A. Loeb, "Direct measurement of cosmological parameters from the cosmic deceleration of extragalactic objects," *Astrophys. J.* **499**, L111–L114 (1998)
4. R. P. Butler, G.W. Marcy, E. Williams, C. McCarthy, P. Dosanjh, S. S. Vogt, "Attaining Doppler Precision of 3 M s^{-1} ," *Astron. Soc. J* **108**, 500-509 (1996)
5. M. T. Murphy, Th. Udem, R. Holzwarth, A. Sismann, L. Pasquini, *et al.*, "High-precision wavelength calibration with laser frequency combs," *Mon. Not. R. Astron. Soc.* **380**, 839–847 (2007)
6. J. Musser, "Novel instrumentation for a scattering independent measurement of the absorption coefficient of natural waters, and a new diffuse reflector for spectroscopic instrumentation and close cavity coupling," PhD thesis (Department of Physics, Texas A&M University, College Station, 2006).

7. P. Eterman, "Integrating cavity spectroscopy," *Appl. Opt.* **9**, 2140-2142 (1970).
8. E. S. Fry, J. Musser, G. W. Kattawar, and P-W Zhai, "Integrating cavities: temporal response," *J. Opt. Soc. Am.* **45**, 9053-9065 (2006).
9. L. Zheng, "Optical absorption of pure water in the blue and ultraviolet," PhD thesis (Department of Physics, Texas A&M University, College Station, 2006).

CONTACT INFORMATION

Name: Juana Gomez

Professional Address: c/o Dr. Edward Fry
Department of Physics and Astronomy
MPY 576
Texas A&M University
College Station, TX 77843

Email Address: jgomezr.12@gmail.com

Education: B.A., Physics, Texas A&M University, May 2010
Undergraduate Research Scholar